Spectrochimica Acta Part A: Molecular and Biomolecular Spectroscopy 128 (2014) 109–118

Contents lists available at ScienceDirect

Spectrochimica Acta Part A: Molecular and Biomolecular Spectroscopy

journal homepage: www.elsevier.com/locate/saa

Vibrational spectroscopy investigation using M06-2X and B3LYP methods analysis on the structure of 2-Trifluoromethyl-10H-benzo[4,5]-imidazo[1,2-a]pyrimidin-4-one

Yusuf Sert [a,b,*], M. Mahendra [c], Chandra [c], K. Shivashankar [d], K.B. Puttaraju [d], H. Doğan [a], Çagrı Çırak [e], Fatih Ucun [f]

[a] Department of Physics, Faculty of Art & Sciences, Bozok University, Yozgat 66100, Turkey
[b] Sorgun Vocational School, Bozok University, Yozgat 66100, Turkey
[c] Department of Studies in Physics, Manasagangotri, University of Mysore, Mysore 570 006, India
[d] P.G. Department of Chemistry, Central College Campus, Bangalore University, Bangalore 560 001, India
[e] Department of Physics, Faculty of Art & Sciences, Erzincan University, Erzincan 24100, Turkey
[f] Department of Physics, Faculty of Art & Sciences, Süleyman Demirel University, Isparta 32100, Turkey

HIGHLIGHTS

- The FT-IR and Laser-Raman spectra of the title compound were recorded in solid phase.
- The optimized geometry and vibrational frequencies were calculated for the first time.
- The HOMO–LUMO energies and related molecular properties were evaluated.

GRAPHICAL ABSTRACT

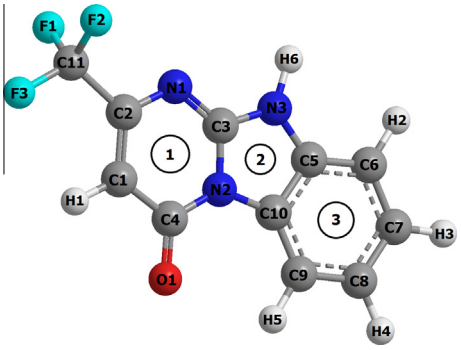

ARTICLE INFO

Article history:
Received 4 January 2014
Received in revised form 1 February 2014
Accepted 19 February 2014
Available online 10 March 2014

Keywords:
FT-IR spectra
Laser-Raman spectra
Vibrational study
Imidazo

ABSTRACT

In this study, the experimental and theoretical vibrational frequencies of a newly synthesized bioactive agent namely, 2-Trifluoromethyl-10H-benzo[4,5]-imidazo[1,2-a]pyrimidin-4-one (TIP) have been investigated. The experimental FT-IR (4000–400 cm^{-1}) and Laser-Raman spectra (4000–100 cm^{-1}) of the molecule in solid phase have been recorded. The theoretical vibrational frequencies and the optimized geometric parameters (bond lengths and bond angles) have been calculated using density functional theory (DFT/B3LYP: Becke, 3-parameter, Lee–Yang–Parr) and M06-2X (the highly parametrized, empirical exchange correlation function) quantum chemical methods with 6-311++G(d,p) basis set by Gaussian 09W software, for the first time. The assignments of the vibrational frequencies have been done by potential energy distribution (PED) analysis using VEDA 4 software. The theoretical optimized geometric parameters and vibrational frequencies have been found to be in good agreement with the corresponding experimental data and results in the literature. In addition, the highest occupied molecular orbital (HOMO) energy, the lowest unoccupied molecular orbital (LUMO) energy and the other related molecular energy values of the compound have been investigated using the same theoretical calculations.

* Corresponding author at: Department of Physics, Faculty of Art & Sciences, Bozok University, Yozgat 66100, Turkey. Tel.: +90 354 2421021; fax: +90 354 2421022.
E-mail address: yusufsert1984@gmail.com (Y. Sert).

http://dx.doi.org/10.1016/j.saa.2014.02.125
1386-1425/

Introduction

Our ongoing research in the field of synthesis and biological evaluation on the dihydrobenzo[4,5]imidazo[1,2-*a*]pyrimidin-4-one fused class of molecules have gained much importance, owing to broad spectrum and wide range of interesting biological activities of the benzimidazole [1,2] and the pyrimidine [3,4]. Hence the fusion of benzimidazole and pyrimidine pharmacophores in a single molecular frame work and its influence on the biological activities are of immense interest; and had become a subject of our study in the recent times. In our previous work [5], we have shown by *in vitro* that the benzo[4,5]imidazo[1,2-*a*]pyrimidin-4-one derivatives have given significant antibacterial, antifungal and anticancer activities and were proven to be highly potent active molecules than the standard drugs available in the market. In view of this background and from the literature survey, which reveals that to the best of our knowledge; the results based on quantum chemical calculations, FT-IR and Laser-Raman spectral studies and HOMO–LUMO analysis on the compound 2-Trifluoromethyl-10H-benzo[4,5]-imidazo[1,2-a]pyrimidin-4-one (TIP) have not been reported elsewhere. Herein, we reported detailed interpretation of the infrared and Raman spectra based on the experimental and theoretical results, which are acceptable and supportable to each other. The structure of title molecule has been also studied by single crystal X-ray diffraction [6]. In this work, the theoretical and experimental studies have been performed to give a detailed definition of the optimized molecular structure and vibrational frequencies of the title molecule.

Experimental details

FT-IR spectrum (4000–400 cm^{-1}) of the title molecule has been recorded by Perkin–Elmer Spectrum Two FT-IR Spectrometer with a resolution of 4 cm^{-1} in solid phase at room temperature. The Raman spectrum has been recorded on Renishaw Invia Raman microscope spectrophotometer in the 4000–100 cm^{-1} region. The excitation line at 785 nm has been taken from a diode laser. Its scan number is 100, the resolution is 1 cm^{-1}, and the sample is in solid phase.

Computational details

Density functional theory (DFT) is an approach to the electronic structure of atoms and molecules and states that all the ground-state properties of a system are function of the charge density. So, DFT calculations cannot be considered a pure *ab initio* method. In DFT, the electron density is the basic variable, instead of the wave function. This reduces the computational burden of treating electron–electron interaction terms, which are treated explicitly as a functional of the density. The DFT approach combines the capacity to incorporate exchange–correlation effects of electrons with reasonable computational costs and high accuracy. The past few years has seen a rapid increase in the use of DFT methods in different types of applications, particularly since the introduction of accurate non-local corrections. In density functional theory, the exchange–correlation energy is the main issue among all of the approximations; therefore, the accuracy of DFT is depended directly by the approximate nature of the exchange–correlation energy functional. The DFT methods employed in the present paper are representative in aspect of the exchange–correlation energy and were commonly used in numerous theoretical studies [7–15].

The high parameterized, empirical exchange correlation functionals, M05-2X and M06-2X, developed by Zhao and Truhlar [16] have been shown to describe noncovalent interactions better than density functionals which are currently in common use. However, these methods have yet to be fully benchmarked for the types of interactions important in biomolecules. M05-2X and M06-2X are claimed to capture "medium-range" electron correlation; however, the "long-range" electron correlation neglected by these functionals can also be important in the binding of noncovalent complex. Also, these methods have been used in numerous theoretical studies, recently [17–23].

Initial atomic coordinates can be generally taken from any database or experimental XRD results. We have used the experimental XRD data and GaussView software database to determine initial atomic coordinates and to optimize the input structure. After the optimization, we have used the most stable optimized structure for other theoretical analysis. In this study, initial atomic coordinates that taken from GaussView database [24] have given most stable structure after optimization. The molecular structure of the title molecule in the ground state (in gas phase) has been optimized by using DFT/B3LYP and M06-2X methods with 6-311++G(d,p) basis set level, and the calculated optimized structure has been used in the vibrational frequency calculations. The calculated harmonic vibrational frequencies have been scaled by 0.9614 (B3LYP) and 0.9489 (M06-2X) for 6-311++G(d,p) level, respectively [24,25]. The same scale factors were used for the entire spectra. The molecular geometry has not been limited, and all the calculations (vibrational wavenumbers, optimized geometric parameters and other molecular properties) have been performed using the Gauss View molecular visualization program [24] and the Gaussian 09W program package on a computing system [26]. Furthermore, the calculated vibrational frequencies have been clarified by means of the potential energy distribution (PED) analysis of all the fundamental vibration modes by using VEDA 4 program [27,28]. VEDA 4 program has been used in previous studies by many researchers [10,15,23,29,30,14]. All the vibrational assignments have been made at B3LYP/6-311++G(d,p) level for which the molecular structure is more stable. So, some assignments may correspond to its previous or next vibrational frequency value at M06-2X/6-311++G(d,p) level.

Results and discussion

Geometric structure

The single crystal X-ray structure analysis of the title compound ($C_{11}H_6F_3N_3O$) showed that its crystal possesses space group C_2/c and belongs to monoclinic system with the following cell dimensions: $a = 20.940$ Å, $b = 13.760$ Å, $c = 7.2852$ Å and, $\beta = 96.369°$ and $V = 2086.2$ Å^3 [6]. The measured density of the molecule is 1.612 mg/m^3. The theoretical and experimental structure parameters (bond lengths and bond angles) are shown in Table 1, in accordance with the atom numbering scheme (the optimized structure) in Fig. 1.

In the title compound, the 2-Trifluoromethyl-10H-benzo[4,5]-imidazo[1,2-a]pyrimidin-4-one,($C_{11}H_6F_3N_3O$), the three fused rings of the benzo[4,5]imidazo[1,2-a]pyrimidine unit are essentially coplanar; the maximum deviation from the mean plane being 0.096 Å. In the crystal, N—H···O hydrogen bonds link the molecules into chains running along the *b*-axis direction [6]. The derivatives of benzopyrimidine are of great importance because of their remarkable biological properties. Some of them have shown good antineoplastic [31] and protein kinase inhibitor [32] activities. Also, heterocycles containing an imidazolone moiety exhibits various biological activities such as antibacterial and antifungal activities [33–35].

In the Ring 1, C—F bond lengths have been observed as experimentally at 1.301–1.328 Å [6], these bond lengths have found 1.348 Å in B3LYP (three bond lengths are same) and changed from

Table 1
Experimental and calculated geometric parameters of the title compound.

Geometric parameters	Experimental values [6]	Calculated values	
Bond lengths (Å)		B3LYP/6-311++G(d,p)	M06-2X/6-311++G(d,p)
C1—C2	1.365	1.367	1.361
C1—C4	1.412	1.444	1.446
C1—H1	0.930	1.079	1.079
C2—N1	1.349	1.358	1.356
C2—C11	1.498	1.519	1.514
C3—N1	1.311	1.303	1.299
C3—N2	1.381	1.380	1.374
C3—N3	1.339	1.365	1.360
C4—N2	1.407	1.430	1.420
C4—O1	1.228	1.217	1.209
C5—C6	1.380	1.389	1.386
C5—C10	1.393	1.406	1.400
C5—N3	1.385	1.392	1.390
C6—C7	1.380	1.394	1.390
C6—H2	0.930	1.083	1.082
C7—C8	1.392	1.400	1.397
C7—H3	0.930	1.083	1.083
C8—C9	1.378	1.394	1.391
C8—H4	0.930	1.083	1.082
C9—C10	1.386	1.389	1.387
C9—H5	0.930	1.080	1.080
C10—N2	1.406	1.406	1.403
N3—H6	0.860	1.007	1.007
C11—F1	1.328	1.348	1.335
C11—F2	1.313	1.348	1.336
C11—F3	1.301	1.348	1.337
R^2		**0.9793**	**0.9767**
Bond angles (°)			
C2—C1—C4	120.6	120.7	120.1
C2—C1—H1	120.0	122.0	122.2
C4—C1—H1	120.0	117.2	117.6
C1—C2—N1	126.1	125.9	126.7
C1—C2—C11	120.6	120.7	120.4
N1—C2—C11	113.3	113.2	112.8
N1—C3—N2	125.6	126.0	126.0
N1—C3—N3	126.8	126.5	126.6
N2—C3—N3	107.5	107.3	107.3
C1—C4—N2	112.8	111.4	111.3
C1—C4—O1	128.3	128.1	128.4
N2—C4—O1	118.9	120.3	120.2
C6—C5—C10	121.5	121.3	121.3
C6—C5—N3	131.0	131.5	131.5
C10—C5—N3	107.5	107.0	107.0
C5—C6—C7	116.7	117.0	116.9
C5—C6—H2	122.0	121.5	121.5
C7—C6—H2	122.0	121.3	121.5
C6—C7—C8	121.8	121.5	121.6
C6—C7—H3	119.0	119.0	119.0
C8—C7—H3	119.0	119.4	119.3
C7—C8—C9	121.8	121.5	121.5
C7—C8—H4	119.0	119.3	119.3
C9—C8—H4	119.0	119.1	119.1
C8—C9—C10	116.4	116.8	116.5
C8—C9—H5	122.0	122.6	122.8
C10—C9—H5	122.0	120.5	120.5
C5—C10—C9	121.9	121.7	121.9
C5—C10—N2	105.8	106.4	106.3
C9—C10—N2	132.3	131.8	131.7
C2—N1—C3	113.4	113.9	113.3
C3—N2—C4	121.4	121.8	122.4
C3—N2—C10	108.9	109.1	109.3
C4—N2—C10	129.7	128.9	128.2
C3—N3—C5	110.2	109.9	109.8
C3—N3—H6	125.0	122.4	122.3
C5—N3—H6	125.0	127.6	127.7
C2—C11—F2	112.3	111.2	111.1
C2—C11—F1	112.8	111.2	110.8
C2—C11—F3	113.7	112.0	111.9
F2—C11—F1	103.8	107.3	107.6
F2—C11—F3	106.7	107.3	107.5
F1—C11—F3	106.9	107.3	107.5
R^2		**0.9747**	**0.9713**

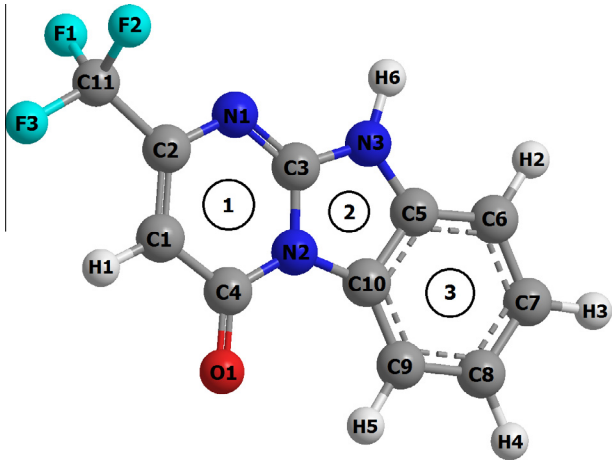

Fig. 1. The optimized molecular structure of the title compound.

1.335 to 1.337 Å in M06-2X methods. These bonds have been reported from 1.3385 to 1.3493 Å in B3LYP/6-311G** and from 1.299 to 1.329 Å in experimentally for (2-trifluoromethyl-5,6,7,8-tetrahydrobenzo[4,5]-thieno[2,3-d]pyrimidin-4-yl)hydrazone monohydrate [36]. Similarly, for 2-amino-4-hydroxy6-trifluoromethylpyrimidine C—F bonds have been calculated from 1.34608 to 1.35258 Å in B3LYP/6-311+G** method [37]. In pyridine ring N1—C2, N1—C3, C3—N2, N2—C4, C4—C1 and C1—C2 bond lengths have been observed 1.349, 1.311, 1.381, 1.407, 1.412 and 1.365 Å, respectively in X-ray study [6]. These bond lengths have been calculated at 1.358/1.356, 1.303/1.299, 1.380/1.374, 1.430/1.420, 1.444/1.446 and 1.367/1.361 Å in B3LYP/M06-2X methods. These bond lengths have been calculated 1.316, 1.346, 1.344, 1.328, 1.383 and 1.408Å, respectively in B3LYP/6-311+G** method [37]. For N1—C2 and N2—C4 bond lengths have been calculated 1.307/1.322 and 1.317/1.334 in HF/B3LYP methods with 6-311++G(d,p) basis set in 2,4-dichloropyrimidine [38]. For 1,2-dihydropyrazolo(4,3-E)pyrimidin-4-one [39] C3—N2, C4—C1 and C1—C2 bond lengths have been calculated 1.26/1.301, 1.336/1.401 and 1.3511/1.442 Å, respectively, in HF/DFT methods with 6-31G(d,p) basis set. In this ring, C4—O1 bond length have been reported as experimentally 1.228 Å [6] and calculated 1.217/1.209 Å in B3LYP/M06-2X methods with 6-311++G(d,p). This bond length have been calculated 1.124/1.4307 Å in HF/DFT methods with 6-31G(d,p) basis set for [1,2-dihydropyrazolo (4,3-E)pyrimidin-4-one [39].

In ring 2, C3—N3, N3—C5, C3—N2 and N2—C10 bond lengths have been reported [6] as 1.339, 1.385, 1.381 and 1.406 Å, respectively. In this study these bond lengths have been calculated 1.365/1.360, 1.392/1.390, 1.380/1.374 and 1.406/1.403 Å, respectively in B3LYP/M06-2X methods. For 2,6-bis(1-benzyl-1H-benzo[d]imidazol-2-yl)pyrimidine [40], these bond lengths were calculated 1.317, 1.378, 1.388 and 1.385 Å, respectively. These bond lengths have been calculated for 2-(thiophene-2-yl)-1H-benzo[d]imidazole(tautomer 1) [41] 1.315, 1.382, 1.383 and 1.384 Å, respectively by using B3LYP/6-311++G(d,p). Additionally, in this study C5—C10 bond length has been calculated 1.406/1.400 Å in B3LYP/M06-2X methods, and this bond length for 2-(thiophene-2-yl)-1H-benzo[d]imidazole(tautomer 1) [41] has been reported as 1.415 Å.

C3—N2—C10 bond angle was calculated 109.1/109.3° in B3LYP/M06-2X methods and observed [6] experimentally as 108.9°. This angle was calculated 105.97° for 2,6-bis(1-benzyl-1H-benzo[d]imidazol-2-yl)pyrimidine [40]. C10—C5—C6 and N2—C3—N3 bond angles have been reported as 121.5° and 107.5° experimentally [6] and calculated 121.3/121.3° and 107.3/107.3° in B3LYP/M06-2X methods. These bond angles have been calculated 120.9°, 121.1°, 121.1°, 121.4° for C10—C5—C6 angle by using different theoretical methods and 110.5° 109.9°, 111.2° and 110.3° for N2—C3—N3 angles with same methods for 2-(1H-imidazo[4,5-f][1,10]phenanthrolin-2yl)phenol [42]. As we can be seen in Table 1 that all of the other distances and angles agree well with the literature. To make comparison with experimental results, we present linear correlation coefficients (R^2) for linear regression analysis of theoretical and experimental bond lengths and angles. These values are 0.9793 and 0.9767 for bond lengths, and 0.9747 and 0.9713 for bond angles with B3LYP and M06-2X. These coefficients can be seen in the last line of Table 1. From these values it can easily be concluded that the geometric parameters calculated with the B3LYP method is much closer to the experimental data.

The largest differences between the calculated (B3LYP/6-311++G(d,p)) and experimental geometries are: 0.032 Å for the C1—C4 bond, 0.021 Å for the C2—C11 bond, 0.026 Å for the C3—N3 bond, 0.023 Å for the C4—N2 bond, 0.147 Å for the N3—H6 bond, 0.047 Å for the C11—F3 bond; 1.4° for the C1—C4—N2 and N2—C4—O1 bond angles, 1.5° for the C10—C9—H5, 2.6° for the C3—N3—H6 and C5—N3—H6, 1.7° for the C2—C11—F3 and 3.5° for the F2—C11—F1 bond angles.

Vibrational analysis

The experimental FT-IR and Laser-Raman spectra of the title compound are compared with the selected theoretical spectra in Figs. 2 and 3, respectively. The scaled calculated harmonic vibrational frequencies at both B3LYP and M06-2X levels, observed vibrational frequencies, and detailed PED assignments are tabulated in Table 2. The harmonic frequencies are calculated for gaseous phase of the isolated title molecule although the experimental ones are obtained for its solid phase. The molecule is interconnected by intermolecular N—H···O hydrogen bonds in solid phase [6]. Consequently, there is slightly disagreement between the observed (experimental) and the calculated frequencies in some modes. So, in order to introduce detailed vibrational assignments of the title molecule, the PED analysis has been carried out. All the calculated modes are numbered from the largest to the smallest frequency within each fundamental wave number.

Ring 1 vibrations

In heterocyclic organic molecules, C—H stretching modes are commonly observed in the region 3500–3000 cm^{-1}. This is the characteristic region for the ready identification of C—H stretching vibration [43]. In this region, the bands are not affected appreciably by nature of the substituents. For 2-amino-4-hydroxy 6-trifluoromethylpyrimidine [37] the band was observed at 3181 cm^{-1}. In the present investigation, the band observed at 3113 cm^{-1} in FT-IR spectrum and this mode was not observed in Laser-Raman spectrum. This mode was calculated at 3116(B3LYP)/3091(M06-2X) cm^{-1}. The C—H bending vibrations (δHCC) are expected to interact a little around 1300–1600 cm^{-1} with ring vibrations [37,43]. In this study, C—H in plane bending vibrations have been observed at 1353(IR)/1373(Ra) and 1246(IR)/1253(Ra) cm^{-1} and calculated at 1345(B3LYP)/1341(M06-2X) and 1232(B3LYP)/1247(M06-2X), respectively. The band at 806 cm^{-1} as associated with C—H out of plane bending mode [37]. In this study, CH out of plane bending modes have been observed at 821(IR)/861(Ra) and 737(IR)/728(Ra) cm^{-1} and calculated at 822(B3LYP)/814(M06-2X) and 742(B3LYP)/745(M06-2X), respectively.

The C=O stretch of carboxylic acids is identical to the C=O stretch in ketones, which is expected in the region 1740–1660 cm^{-1} [44]. This band is reasonably easy to be recognized due to its high intensity. For 9-[(2-hydroxyethoxy)methyl] guanine [45] the band were observed at 1633 and 1632 cm^{-1} in FT-IR and FT-Raman spectra. In this study C=O stretching modes have

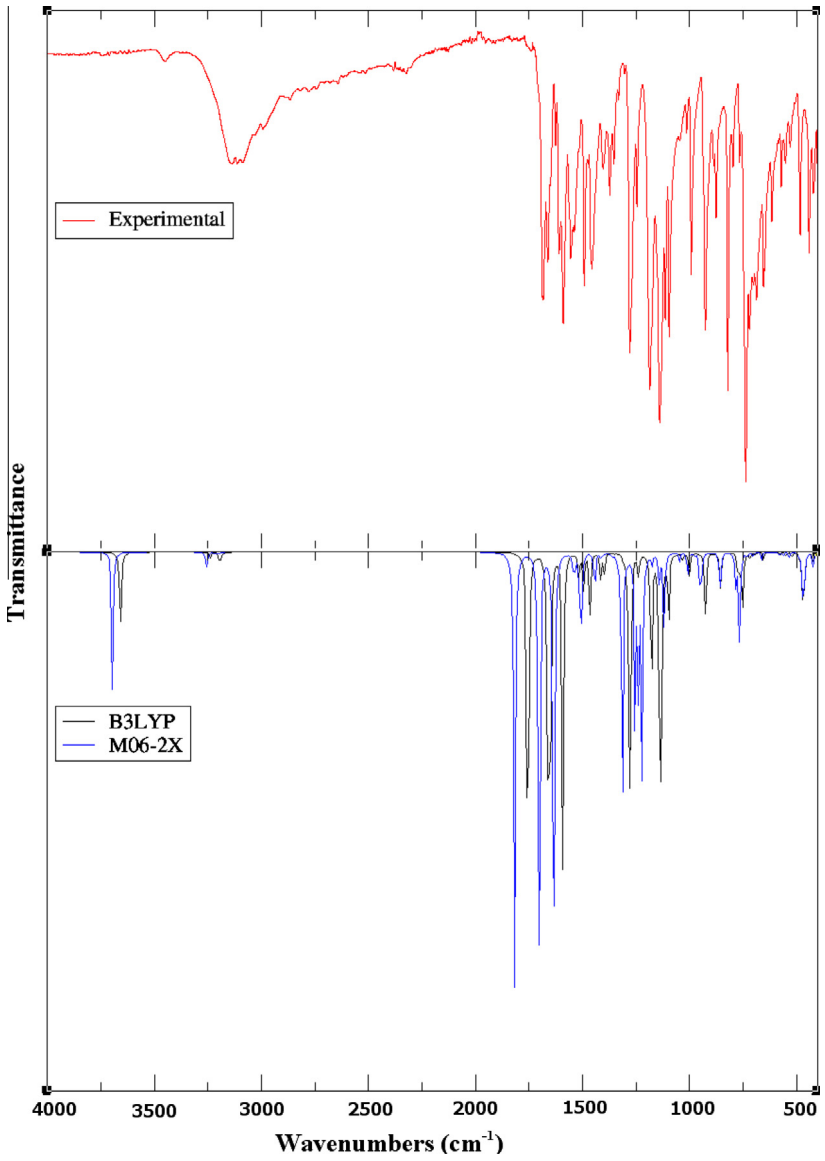

Fig. 2. Comparison of observed and calculated infrared spectra of the title compound.

been observed at 1684(IR)/1674 (Raman) and calculated at 1689(B3LYP)/1725(M06-2X) cm^{-1}. In plane bending δOCC (O1—C4—C1) modes have been observed at 615(IR)/661(Ra), 403 cm^{-1} in FT-IR and 345 cm^{-1} in Laser-Raman spectra and calculated at 630(B3LYP)/630(M06-2X), 398(B3LYP)/396(M06-2X) and 331(B3LYP)/334(M06-2X), respectively. Out of plane γONCC (O1—N2—C4—C1) modes have been observed 821(IR)/861(Ra), 737(IR)/728(Ra), 687(IR)/694(Ra) and 655(IR)/661(Ra) cm^{-1} and calculated in υ36, υ37, υ42 and υ44 modes.

Pyrimidines absorb strongly in the region 1600-1500 cm^{-1} due to the C=C (C2=C1) and C=N (N1=C3) ring stretching vibrations [46,47]. C2=C1 modes have been observed at 1609(IR)/1612(Ra), 1590(IR)/1588(Ra) and 1556(IR)/1559(Ra) cm^{-1} and N1=C3 stretching modes have been observed at 1609(IR)/1612(Ra) and 1590(IR)/1588(Ra) cm^{-1}. These stretching modes are agreed with theoretical values and this agreement can be seen in Table 2. The identification of C=N vibrations is a difficult task, since the mixing of vibrations is possible in this region. The unconjucated C=N linkage in the amine gives medium to weak bands near 1250–1020 cm^{-1} [47]. C=N modes have been observed at 1404(IR)/1411(Ra), 1373(IR)/1373(Ra), 1139(IR)/1148(Ra) and 1047(IR)/1029(Ra) cm^{-1} and these modes agreed with the theoretical calculations (υ14, υ15, υ24 and υ28).

Usually symmetric and antisymmetric CF_3 vibrations are in the ranges 1270–1235 and 1226–1200 cm^{-1}, respectively [48,49]. In this study, there are nine stretching CF_3 modes. These are four symmetric and five asymmetric modes. Symmetric modes were observed at 1246(IR)/1253(Ra), 890(IR)/876(Ra), 721(IR)/728(Ra) and 687(IR)/694(Ra) cm^{-1} and asymmetric stretching modes were observed at 1139(IR)/1148(Ra), 1113(IR)/1091(Ra), 1095(IR)/1091(Ra), 530(Ra) and 506(Ra) cm^{-1}. These modes agree with theoretical values and this agreement can be seen in Table 2. For 2-amino4-hydroxy6-trifluoromethylpyrimidine [37], these modes are compatible with our modes values. The other wave numbers of the trifluoromethyl group such as symmetric modes (υ19, υ40, υ41 and υ43), asymmetric modes (υ25), out of plane modes γFCFC (υ26, υ49, υ50, υ56, υ57, υ60, υ62 and υ63), twisting modes (υ50, υ51, υ54, υ55, υ56, υ57, υ59) and rocking modes (υ49) are also assigned and presented in Table 2. These assignments are substantiated by the reported literatures of similar kind of molecules.

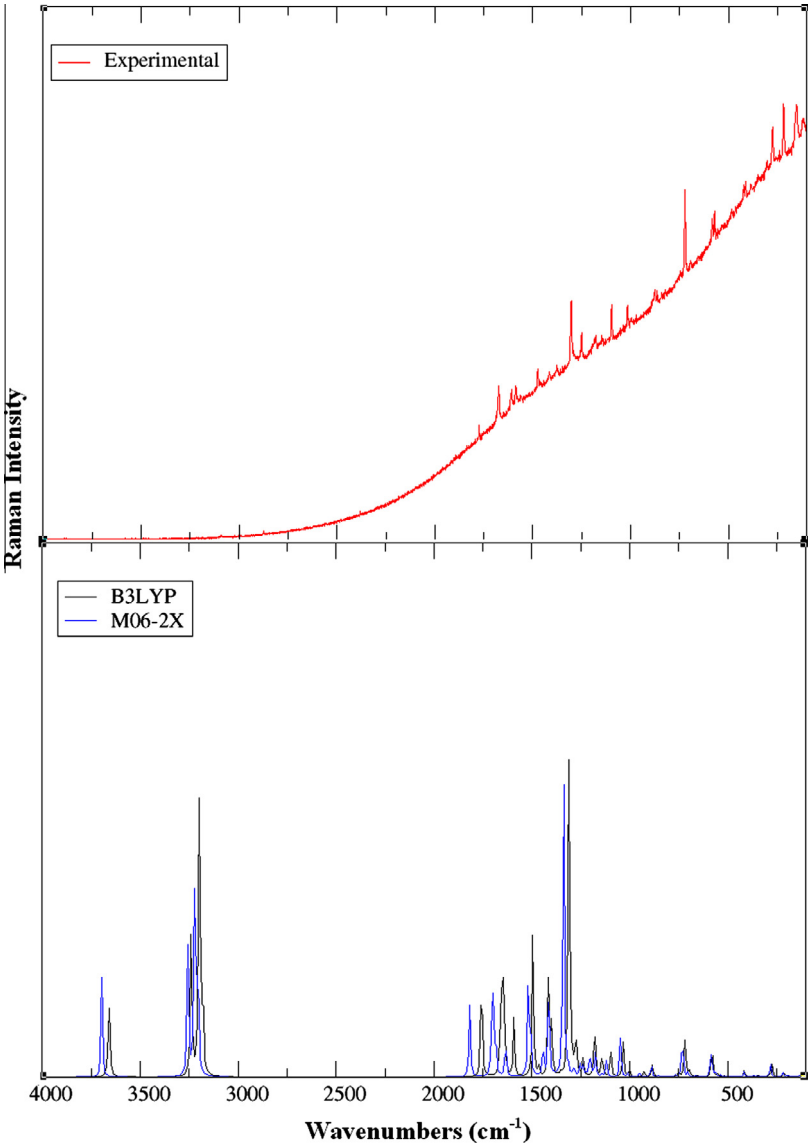

Fig. 3. Comparison of observed and calculated Raman spectra of the title compound.

Ring 2 vibrations

It has been observed that the presence of N—H in various molecules may be correlated with a constant occurrence of absorption bands whose positions are slightly altered from one compound to another; this is because the atomic group vibrates independently of the other groups in the molecule and has its own frequency. In all the heterocyclic compounds, the N—H stretching vibrations occur in the region 3500–3000 cm^{-1} [50]. In this study N—H (N3—H6 in the ring 2) stretching mode was observed at 3456 cm^{-1} in FT-IR spectrum, but this mode was not observed in Laser-Raman spectrum, which is further supported by the PED contribution of 100%. This mode was calculated at 3518(B3LYP)/3507(M06-2X) cm^{-1} with 6-311++G(d,p) basis set. By Arivazhagan et al. [51], N—H stretching vibrations have been found at 3258, 3210, 3116 cm^{-1} in IR and 3132 cm^{-1} in Raman spectrum for xanthenes. The in-plane bending δHNC modes have been observed at 1373(IR)/1373(Ra), 1329(IR)/1296(Ra), 1246(IR)/1253(Ra) and 1185(IR)/1182(Ra) cm^{-1} and calculated at 1361(B3LYP)/1370(M06-2X), 1300(B3LYP)/1288(M06-2X), 1224(B3LYP)/1219(M06-2X) and 1191(B3LYP)/1191(M06-2X), respectively. The out of plane modes (τHNCN) have been observed at 441(IR)/422(Ra) and 403(IR)/407(Ra) cm^{-1}, and calculated at 451(B3LYP)/445(M06-2X) and 407(B3LYP)/402 (M06-2X) cm^{-1}, respectively. The in-plane and out of plane bending vibrations of N—H group are also supported by the literature [51,52].

In ring 2, other related modes are υNC stretching modes (υ15:N2—C3, υ21:N3—C5 and υ23:N3—C3), bending modes δCNC (υ16:C3—N3—C5 and υ18:N2—C3—N3) and δNCN (υ63:N2—C3—N3), torque modes τCCNC (υ39:C10—C5—N3—C3) and τCNCN (υ:64:C2—N1—C3—N3) and out of modes γNNNC (υ44:N1—N2—N3—C3). These modes of ring 2 are also supported by the literature [51,52].

Ring 3 vibrations

Aromatic compounds commonly exhibit multiple weak bands in the region 3100–3000 cm^{-1} due to aromatic C—H stretching vibrations which is the characteristic region for ready identification of this structure [53–56]. In this region, the bands are not affected appreciably by nature of the substituent. In this study, there are two symmetric and two asymmetric stretching modes. The symmetric stretching mode was observed at 3113 cm^{-1} in FT-IR spectrum. The asymmetric mode was observed 3086 cm^{-1} in

Table 2
Observed and calculated vibrational frequencies of the title compound with 6—311++G(d,p).

Vibration no.	Assignments	Observed frequencies		Calculated frequencies in cm^{-1}	
		FT-IR	Laser-Ra.	B3LYP	M06-2X
ν_1	υNH(100) in the N3—H6 (ring 2)	3456		3518	3507
ν_2	υCH(100) in the C1—H1 (ring 1)	3113		3116	3091
ν_3	υCH(98) in the ring 3	3113		3112	3088
ν_4	υCH(94) in the ring 3	3086		3076	3057
ν_5	υCH(94) in the ring 3	3086		3067	3047
ν_6	υCH(95) in the ring 3	3086		3055	3037
ν_7	υOC(64) in the O1—C4 + δCNC(14) in the C4—N2—C3	1684	1674	1689	1725
ν_8	υCC(34) in the C5—C6,C8—C9,C1—C2 + υNC(15) in the N1—C3	1609	1612	1598	1618
ν_9	υNC(27) in the N1—C3 + υCC(22) in the C5—C6, C2—C1	1590	1588	1588	1611
ν_{10}	υCC(54) in the C7—C8 + δCCC(12) in the C5—C6—C7	1590	1588	1576	1597
ν_{11}	υCC(57) in the C1—C2	1556	1559	1531	1552
ν_{12}	δHCC(33) in the ring 3 + υCC(25) in the C8—C9	1456	1478	1459	1461
ν_{13}	δHCC(36) in the ring 3 + δCCC(27) in the C7—C8—C9	1456	1478	1438	1440
ν_{14}	υNC(29) in the N1—C2 + δCCN(15) in the C1—C2—N1	1404	1411	1409	1430
ν_{15}	υNC(34) in the N2—C3 + υCC(14) in the C7—C8 + δHNC(13) in the H6—N3—C3	1373	1373	1361	1370
ν_{16}	υCC(11) in the C7—C8 + δHCC(11) in the ring1 and ring 3 + δCNC(10) in the C3—N3—C5	1353	1373	1345	1341
ν_{17}	δHCC(25) in the ring 3 + δHNC(11) in the H6—N3—C3 + υCC(11) in the C9—C10	1329	1296	1300	1288
ν_{18}	υCC(14) in the C8—C9 + δNCN(13) in the N2—C3—N3	1279	1253	1259	1269
ν_{19}	δHCC(41) in the ring 1 + υCC(18) in the C2—C11 + υFC(13) in the F2—C11 + δFCF(11) in the F1—C11—F3	1246	1253	1232	1247
ν_{20}	δHNC(17) in the H6—N3—C3 + δHCC(12) in the ring 3	1246	1253	1224	1219
ν_{21}	υNC(27) in the N3—C5 + δHNC(15) in the H6—N3—C5	1185	1182	1191	1191
ν_{22}	δHCC(47) in the ring 3 + υCC(10) in the C1—C4	1139	1148	1137	1176
ν_{23}	υFC(19) in the F—C11 + δHCC(12) in the ring 3 + υNC(10) in the N3—C3	1139	1148	1134	1160
ν_{24}	υNC(27) in the N2—C4 + δHCC(25) in the ring 1 and ring 3	1139	1148	1131	1142
ν_{25}	δFCF(48) in the F—C11—F + υFC(45) in the F—C11	1113	1091	1098	1119
ν_{26}	υFC(79) in the F—C11 + γFCFC(14) in the F1—C11—F3—C2	1095	1091	1089	1115
ν_{27}	δHCC(36) in the ring 3 and ring 1	1095	1091	1088	1084
ν_{28}	υNC(35) in the N1—C2 + δHCC(10) in the ring 1	1047	1029	1056	1062
ν_{29}	υCC(37) in the C7—C8 + δHCC(15) in the ring 3	993	1029	994	995
ν_{30}	δCCN(17) in the C1—C4—N2 + δCCC(13) in the C8—C9—C10 + δNCN(12) in the N1—C3—N2 + υNC(12) in the N1—C2	993	971	963	959
ν_{31}	τHCCC(71) in the ring 3 out of H + τCCNC(12) in the C6—C5—N3—C3	926	971	953	958
ν_{32}	τHCCC(73) in the RİNG 3 out of H	926	971	918	927
ν_{33}	υFC(22) in the F—C11 + δCNC(21) in the C2—N1—C3	890	876	890	900
ν_{34}	δCCC(42) in the C7—C8—C9	876	861	851	845
ν_{35}	τHCCC(76) in the ring 3 out of H	821	861	833	840
ν_{36}	τHCCC(75) in the ring 1 out of H + γONCC(13) in the O1—N2C4—C1	821	861	822	814
ν_{37}	τHCCC(28) in the ring 1 and ring 3 out of H + γNNNC(20) in the N1—N2—N3—C3 + γONCC(12) in the O1—N2C4—C1 + γCCNC(10) in the C1—C2—N1—C3	737	728	742	745
ν_{38}	τHCCC(33) in the ring 3 out of H + τCCCC(14) in the C5—C6—C7—C8 + γCCCN(11) in the C8—C9—C10—N2	721	728	727	729
ν_{39}	τCCNC(19) in the C10—C5—N3—C3 + τHCCC(18) in the ring 3 out of H + τCCCC(12) in the C8—C9—C10—C5	721	728	723	727
ν_{40}	υFC(21) in the F—C11 + δCCC(12) in the C9—C10—C5 + δFCF(12) in the F—C11—F	721	728	721	716
ν_{41}	δCCC(17) in the C9—C10—C5 + δFCF(13) in the F—C11—F + υFC(11) in the F—C11	687	694	690	694
ν_{42}	γONCC(57) in the O1—N2—C4—C1 + γCCNC(16) in the C1—C4—N2—C3	687	694	688	691
ν_{43}	δNCN(18) in the N2—C3—N3 + δFCF(14) in the F—C11—F + δCCN(10) in the C10—C5—N3	655	694	667	667
ν_{44}	γNNNC(40) in the N1—N2—N3—C3 + γONCC(18) in the O1—N2—C4—C1 + γCCNC(11) in the C1—C4—N2—C3	655	661	664	665
ν_{45}	δCNC(18) in the C3—N2—C4 + δOCC(14) in the O1—C4—C1 + δNCN(12) in the N1—C3—N2	615	661	630	630
ν_{46}	δCCC(30) in the C6—C5—C10 + δCCN(13) in the C1—C2—N1	553	570	558	556
ν_{47}	γCCCN(24) in the C7—C6—C5—N3 + τHCCC(19) in the ring 3out of H + τCCNC(17) in the C10—C5—N3—C3 + τCCCC(14) in the C6—C7—C8—C9	553		555	551
ν_{48}	δCNC(21) in the C2—N1—C3 + υNC(12) in the N2—C3	553		554	551
ν_{49}	δFCF(23) in the F—C1—F + γFCFC(20) in the F1—C11—F3—C2 + υFC(12) in the F—C11	530		529	534
ν_{50}	δFCF(48) in the F—C11—F + γFCFC(13) in the F1—C11—F3—C2 + υFC(11) in the F—C11	506		502	509
ν_{51}	δFCF(23) in the F—C11—F + υNC(11) in the N2—C3	483	479	467	466
ν_{52}	τHNCN(61) in the ring 2 out of H	441	422	451	445
ν_{53}	τCCNC(31) in the C6—C5—N3—C3 + τHNCN(28) in the ring 2 out of H + τCNCC(11) in the C3—N2—C10—C9	403	407	407	402
ν_{54}	υNC(14) in the N2—C4 + υCC(11) in the C5—C10 + δOCC(11) in the O1—C4—C1 + δCNC(11) in the C4—N2—C10 + δFCF(11) in the F—C11—F	403	407	398	396
ν_{55}	τCNCC(17) in the C3—N2—C10—C9 + δFCF(15) in the F—C11—F + γCCCN(14) in the C7—C6—C5—N3		345	351	349
ν_{56}	δFCF(29) in the F—C11—F + δOCC(17) in the O1—C4—C1 + γFCFC(20) in the F1—C11—F3—C2		345	331	334
ν_{57}	γFCFC(24) in the F1—C11—F3—C2 + γNNNC(13) in the N1—N2—N3—C3 + τCNCC(13) in the C3—N1—C2—C1 + δFCF(11) in the F—C11—F		278	279	278
ν_{58}	τCCNC(41) in the C9—C10—N2—C3 + γCCCN(23) in the C7—C6—C5—N3 + τCNCN(17) in the C10—N2—C3—N1		278	268	266
ν_{59}	υCC(28) in the C2—C11 + δCNC(14) in the C2—N1—C3 + δFCF(14) in the F—C11—F		278	262	265
ν_{60}	δCCN(18) in the C9—C10—N2 + δCNC(16) in the N1—C3—N2 + γFCFC(24) in the F1—C11—F3—C2		216	205	206
ν_{61}	τCNCN(40) in the C4—N2—C3—N1 + τCCNC(28) in the C1—C2—N1—C3		154	190	186
ν_{62}	τCNCC(31) in the C10—N2—C4—C1 + τCCNC(25) in the C1—C2—N1—C3 + γFCFC(13) in the F1—C11—F3—C2		154	130	129

(*continued on next page*)

Table 2 (*continued*)

Vibration no.	Assignments	Observed frequencies		Calculated frequencies in cm^{-1}	
		FT-IR	Laser-Ra.	B3LYP	M06-2X
ν_{63}	δCCN(50) in the C11—C2—N1 + γFCFC(13) in the F1—C11—F3—C2 + δNCN(12) in the N2—C3—N3		116	126	126
ν_{64}	γCCCN(62) in the C2—C1—C4—N2 + τCNCC(11) in the C4—N2—C10—C5 + τCNCN(10) in the C2—N1—C3—N3		116	110	111
ν_{65}	τCNCC(25) in the C3—N1—C2-C11 + τCCNC(13) in the C6—C5—N3—C3 + γCCNC(12) in the C9—C10—N2—C4 + γNNNC(10) in the N1—N2—N3—C3			48	47
ν_{66}	τFCCC(90) in the F1,F2,F3—C11—C2—C1			26	27
R^2				0.9996	0.9993

υ, stretching; δ, in-plane bending; γ, out-of-plane bending; τ, torsion.
Potential energy distribution (PED), less than 10% are not shown.

FT-IR spectrum. However, these modes have not been observed in Laser-Raman spectrum. Theoretical symmetric modes have been calculated at 3112/3088 and 3076/3057 cm^{-1} in B3LYP/M06-2X methods. Theoretical asymmetric stretching modes have been calculated at 3067/3047 and 3055/3037 with same methods. Substitution sensitive C—H plane bending vibrations lie in the region 1300–1000 cm^{-1} [47]. In this study in-plane bending vibrations have been observed at 1456(IR)/1478(Ra), 1353(IR)/1373(Ra), 1329(IR)/1296(Ra), 1246(IR)/1253(Ra), 1139(IR)/1148(Ra), 1095(IR)/1091(Ra) and 993(IR)/1029(Ra) cm^{-1}. These modes have been calculated at 1459/1461, 1438/1440, 1345/1341, 1300/1288, 1224/1219, 1137/1176, 1131/1142, 1088/1084 and 994/995 cm^{-1} in B3LYP/M06-2X methods. Band involving the out of plane C—H vibrations appear in the range 1000–675 cm^{-1} [47]. In this study, out of plane vibrations have been observed at 926(IR)/971(Ra), 821(IR)/861(Ra), 737(IR)/728(Ra) and 553(Ra) cm^{-1}, and calculated at 953/958, 918/927, 833/840, 742/745, 727/729, 723/727 and 555/551 cm^{-1} in B3LYP/M06-2X methods with 6-311++G(d,p) basis set.

The ring carbon–carbon stretching vibrations occur in the region 1625–1430 cm^{-1}. In general, the bands are of variable intensity and are observed at 1625–1590, 1590–1575, 1540–1470, and 1465–1430 and 1380–1280 cm^{-1} from the wavenumber ranges given [56–59]. In the present work, the wavenumbers observed in

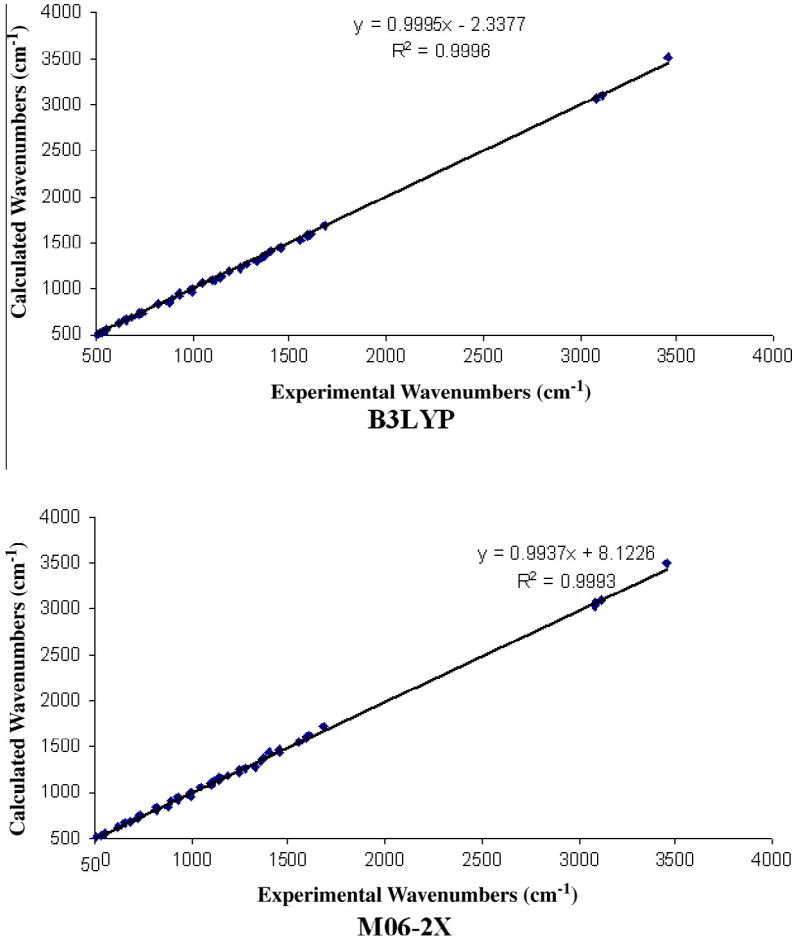

Fig. 4. Correlation graphics of experimental and theoretical (scaled) wavenumbers of the title compound.

FT-IR/Laser-Raman spectra at 1609/1612, 1590/1588, 1456/1478, 1373/1373, 1353/1373, 1329/1296, 1279/1253 and 993/1029 cm^{-1} have been assigned to C—C stretching vibrations. The theoretical computed values in B3LYP/M06-2X at 15978/1618, 1588/1611, 1576/1597, 1459/1461, 1361/1370, 1345/1341, 1300/12881259/1269 and 994/995 cm^{-1} (nine bands). The PED corresponding to all C—C vibrations lies between 11% and 54% as shown in Table 2. These C—C stretching modes have been observed at 1589 and 1516 cm^{-1} in FT-IR and 1596 and 1541 cm^{-1} in FT-Raman spectra by Rofouei et al. [57]. All these calculated values are in good agreement with the experimental data. The remainder of the observed and calculated wavenumbers and assignments of present molecule are shown in Table 2.

The correlation graphic which describes harmony between the calculated and experimental wavenumbers is shown in Fig. 4. As can be seen from Fig. 4, the experimental fundamentals have good correlation with B3LYP. The relations between the calculated and experimental wavenumbers are linear and described by the following equation:

$$\upsilon_{Cal} = 0.9995\ \upsilon_{exp} - 2.3377 \text{ for B3LP method}$$
$$\upsilon_{Cal} = 0.9937\ \upsilon_{exp} + 8.1226 \text{ for M06-2X method}$$

We calculated R^2 values (R^2 = 0.9996 for B3LYP and R^2 = 0.9993 for M06-2X) between the calculated and experimental wavenumbers. As a result, the performances of the B3LYP method with respect to the prediction of the wavenumbers within the molecule were quite close.

Homo–Lumo analysis

Many organic molecules containing conjugated π electrons have been characterized as hyperpolarizabilities and researched by means of vibrational spectroscopy. The π electron cloud moment from donor to acceptor can make the molecule highly polarized through the single-double path when it changes from the ground state to the excited state. Both the highest occupied molecular orbital (HOMO) and the lowest unoccupied molecular orbital (LUMO) are the main orbitals taking part in chemical stability. The HOMO represents the ability to donate an electron, LUMO as an electron acceptor represents the ability to obtain an electron [60]. The LUMO and HOMO energies have been calculated by

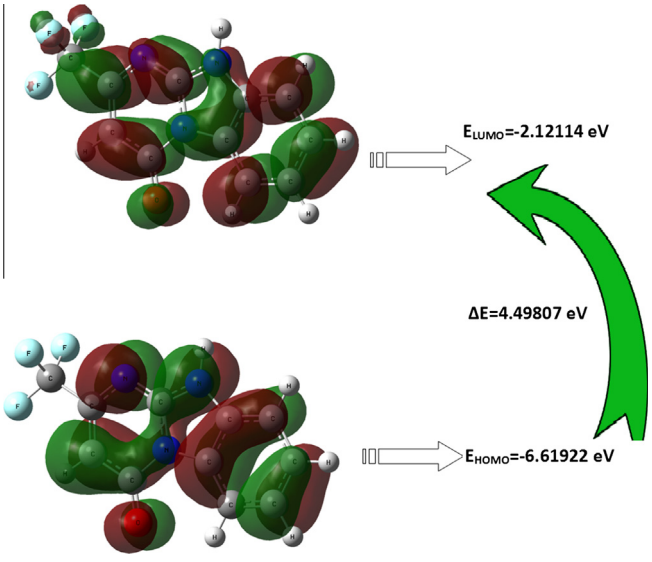

Fig. 5. Calculated HOMO–LUMO plots of the title compound.

Table 3
Comparison of HOMO–LUMO energy gaps and related molecular properties of the title compound.

Molecular properties	B3LYP/6-311++G(d,p)	M06-2X/6-311++G(d,p)
Energies (a.u)	−962.09895620	−961.75930183
E_{HOMO} (eV)	−6.61922	−7.82496
E_{LUMO} (eV)	−2.12114	−1.11132
Energy Gap (eV)	4.49807	6.71364
Ionization potential (I)	6.61922	7.82496
Electron affinity (A)	2.12114	1.11132
Global hardness (η)	2.24903	3.35682
Chemical potential (μ)	4.37018	4.46814
Electrophilicity (ψ)	4.24500	2.97150
Softness (ζ)	0.44463	0.29790
Dipol moment (debye)	6.0886	5.9677

B3LYP/6-311++G(d,p) and M06-2X/6-311++G(d,p) methods, and depicted in Fig 5. Considering the chemical hardness, large HOMO–LUMO gap means a hard molecule and small HOMO–LUMO gap means a soft molecule. One can also relate the stability of the molecule to hardness, which means that molecule with least HOMO–LUMO gap means it is more reactive [61]. The frontier molecules orbital, HOMO and LUMO and frontier orbital energy gap helping to exemplify the reactivity and kinetic stability of molecules are important parameters in the electronic studies [62,63]. The analysis of the wave function indicates that the electron absorption corresponding to the transition from the ground state to the first excited state is mainly defined by one electron excitation from the highest occupied orbital (HOMO) to the lowest unoccupied orbital (LUMO) [64].

The calculated energy of the title compound is −962.09895620 a.u in B3LYP/6-311++G(d,p) and −961.75930183 a.u in M06-2X/6-311++G(d,p). Meanwhile, the lowering of the energy gap describes that the eventual charge transfer takes place within the molecule. The HOMO–LUMO energy gap calculated at B3LYP and M06-2X/6-311++G(d,p) level reflect the chemical activity of the molecule and explain the eventual charge transfer interaction within the molecule, which influences the biological activity of the molecule. The positive phase is represented in red color and the negative phase is represented in green color. HOMO–LUMO plots are shown in Fig. 5. As seen from the figures, the HOMO is located on ring 1, ring 2 and ring 3, but on CF_3 group was not observed, the LUMO is more focused on all of the molecules.

Associated within the framework of molecular orbital theory, the ionization energy and electron affinity can be expressed by HOMO and LUMO orbital energies as $I = -E_{HOMO}$ and $A = -E_{LUMO}$. The global hardness, $\eta = 1/2(E_{LUMO} - E_{HOMO})$. The electron affinity can be used in combination with ionization energy to give electronic chemical potential, $\mu = 1/2(E_{LUMO} + E_{HOMO})$. The global electrophilicity index, $\psi = \mu^2/2\eta$ and softness, $\zeta = 1/\eta$ [65,66]. These parameters have been evaluated and tabulated in Table 3.

Conclusion

In this study, the vibrational analysis of a newly synthesized bioactive agent, 2-Trifluoromethyl-10H-benzo[4,5]-imidazo[1,2-a]pyrimidin-4-one molecule has been studied by experimental (FT-IR and Laser-Raman spectra) and theoretical (DFT/B3LYP and M06-2X) methods. The optimized geometric parameters, vibrational harmonic frequencies, PED assignments, molecular orbital energies and other properties (related with HOMO and LUMO energy values) of the compound have been calculated by using DFT/B3LYP and M06-2X methods with 6-311++G(d,p) basis set. The theoretical optimized geometric parameters (bond lengths and angles) and vibrational frequencies are compared with the experimental data. Considerable level of correlation has been

noticed. The detailed PED% analysis of the compound showed a good agreement with the experimental data. The calculated HOMO and LUMO along with their plot has been presented for understanding of charge transfer occuring within the molecule. These results are taken into account; we conclude that the title compound is an attractive object for future medicinal and pharmacological studies to evaluate its therapeutical importance.

References

[1] Y. Li, C. Tan, C. Gao, C. Zhang, X. Luan, X. Chen, H. Liu, Y. Chen, Y. Jiang, Bioorg. Med. Chem. 19 (2011) 4529–4535.
[2] K. Starcevic, M. Kralj, K. Ester, I. Sabol, M. Grec, K. Pavelic, G.K. Zamola, Bioorg. Med. Chem. 15 (2007) 4419–4426.
[3] T. Gazivoda, M. Sokcevic, M. Kralj, L. Suman, K. Pavelic, E.D. Clercq, G. Andrei, R. Snoeck, J. Balzarini, M. Mintas, S.R. Malic, J. Med. Chem. 50 (2007) 4105–4112.
[4] S. Noll, M. Kralj, L. Suman, H. Stephan, I. Piantanid, Eur. J. Med. Chem. 44 (2009) 1172–1179.
[5] K.B. Puttaraju, K. Shivashankar, Chandra, M. Mahendra, V.P. Rasal, P.N. Venkatavivek, N. Ponnuru, K. Rai, M.B. Chanu, Eur. J. Med. Chem. 69 (2013) 316–322.
[6] Chandra, K.B. Puttaraju, K. Shivashankar, E.A. Jithesh Babu, M. Mahendra, Acta Cryst. E69 (2013) o1536.
[7] M.A. Palafox, V.K. Rastogi, R.P. Tanwar, L. Mittal, Spectrochim. Acta A 59 (2003) 2473–2486.
[8] S. Mohan, N. Sundaraganesan, J. Mink, Spectrochim. Acta A 47 (1991) 1111–1115.
[9] G.N. Ten, V.V. Nechaev, A.N. Pankratov, V.I. Berezin, V.I. Baranov, J. Struct. Chem. 51 (2010) 854–861.
[10] Ç. Çırak, N. Koç, J. Mol. Model 18 (2012) 4453–4464.
[11] M.A. Palafox, G. Tardajos, A. Guerrero-Martinez, V.K. Rastogi, D. Mishra, S.P. Ojha, W. Kiefer, Chem. Phys. 340 (2007) 17–31.
[12] M. Szczesniak, M.J. Nowak, K. Szczepaniak, W.B. Person, Spectrochim. Acta A 41 (1985) 237–250.
[13] J.S. Singh, J. Mol. Struct. 876 (2008) 127–133.
[14] M.H. Jamróz, J.C. Dobrowolski, R. Brzozowski, J. Mol. Struct. 787 (2006) 172–183.
[15] Ç. Çırak, Y. Sert, F. Ucun, Spectrochim. Acta A 92 (2012) 406–414.
[16] Y. Zhao, D.G. Truhlar, Theor. Chem. Account. 120 (2008) 215–241.
[17] K. Helios, R. Wysokiński, A. Pietraszko, D. Michalska, Vib. Spectrosc. 55 (2011) 207–215.
[18] J. Gu, J. Wang, J. Leszczynski, Chem. Phys. Lett. 512 (2011) 108–112.
[19] K.H. Lemke, T.M. Seward, Chem. Phys. Lett. 573 (2013) 19–23.
[20] E.I. Paulraj, S. Muthu, Spectrochim. Acta A 108 (2013) 38–49.
[21] U. Yadava, M. Singh, M. Roychoudhury, Comput. Theor. Chem. 977 (2011) 134–139.
[22] C.N. Ramachandran, E. Ruckenstein, Comput. Theor. Chem. 973 (2011) 28–32.
[23] Y. Sert, Ç. Çırak, F. Ucun, Spectrochim. Acta A 107 (2013) 248–255.
[24] A. Frish, A.B. Nielsen, A.J. Holder, Gauss View User Manual, Gaussian Inc., Pittsburg, PA, 2001.
[25] W.H. James, E.G. Buchanan, C.W. Müller, J.C. Dean, D. Kosenkov, L.V. Slipchenko, L. Guo, A.G. Reidenbach, S.H. Gellman, T.S. Zwier, J. Phys. Chem. A115 (2011) 13783–13798.
[26] M.J. Frisch, G.W. Trucks, H.B. Schlegel, G.E. Scuseria, M.A. Robb, J.R. Cheeseman, G. Scalmani, V. Barone, B. Mennucci, G.A. Petersson, H. Nakatsuji, M. Caricato, X. Li, H.P. Hratchian, A.F. Izmaylov, J. Bloino, G. Zheng, J.L. Sonnenberg, M. Hada, M. Ehara, K. Toyota, R. Fukuda, J. Hasegawa, M. Ishida, T. Nakajima, Y. Honda, O. Kitao, H. Nakai, T. Vreven, J.A. Montgomery Jr., J.E. Peralta, F. Ogliaro, M. Bearpark, J.J. Heyd, E. Brothers, K.N. Kudin, V.N. Staroverov, R. Kobayashi, J. Normand, K. Raghavachari, A. Rendell, J.C. Burant, S.S. Iyengar, J. Tomasi, M. Cossi, N. Rega, J.M. Millam, M. Klene, J.E. Knox, J.B. Cross, V. Bakken, C. Adamo, J. Jaramillo, R. Gomperts, R.E. Stratmann, O. Yazyev, A.J. Austin, R. Cammi, C. Pomelli, J.W. Ochterski, R.L. Martin, K. Morokuma, V.G. Zakrzewski, G.A. Voth, P. Salvador, J.J. Dannenberg, S. Dapprich, A.D. Daniels, Ö. Farkas, J.B. Foresman, J.V. Ortiz, J. Cioslowski, D.J. Fox, Gaussian 09, Revision A1, Gaussian, Inc., Wallingford CT, 2009.
[27] M.H. Jamróz, Vibrational Energy Distribution Analysis VEDA 4, Warsaw, 2004.
[28] M.H. Jamróz, Spectrochim. Acta A 114 (2013) 220–230.
[29] H. Arslan, Ö. Algül, Spectrochim. Acta A 70 (2008) 109–116.
[30] Ç. Çırak, S. Demir, F. Ucun, O. Çubuk, Spectrochim. Acta A 79 (2011) 529–532.
[31] A.A.M. Abdel-Hazel, Arch. Pharm. Res. 30 (2007) 678–684.
[32] J.J. Nunes, X.T. Zhou, P. Amouzeng, C. Ghiron, D.N. Johnston, E.C. Power, WO Patent No. 2 005 009 443, 2005.
[33] F. Palacious, C. Alanso, D. Aparicio, G. Rubiales, J.M. Santos, Tetrahedron 63 (2007) 523–575.
[34] E. Duval, A. Case, R.L. Stein, G.D. Cunny, Bioorg. Med. Chem. Lett. 15 (2005) 1885–1889.
[35] M.B. Teimouria, R. Bazhrang, Bioorg. Med. Chem. Lett. 16 (2006) 3697–3701.
[36] Y. Ping, W. Yan, D. Zheng-Chao, S. Yu, N. Guang-Hua, S. Xin-Jian, T. Da-Ting, Chinese J. Struct. Chem. 32 (2013) 1023–1030.
[37] V. Krishnakumar, N. Prabavathi, Spectrochim. Acta A 71 (2008) 449–457.
[38] U. Rani, H. Oturak, S. Sudha, N. Sundaraganesan, Spectrochim. Acta A 78 (2011) 1467–1475.
[39] G. Ramachandran, S. Muthu, J.U. Maheswari, Solid State Sci. 16 (2013) 45–52.
[40] E. İnkaya, S. Günnaz, N. Özdemir, O. Dayan, M. Dinçer, B. Çetinkaya, Spectrochim. Acta A 103 (2013) 255–263.
[41] A. Ünal, B. Eren, Spectrochim. Acta A 114 (2013) 129–136.
[42] T. Tang, G. Tang, S. Kou, J. Zhao, L.F. Culnane, Y. Zhang, Spectrochim. Acta A 117 (2014) 144–151.
[43] S. Ramalingam, S. Periandy, S. Mohan, Spectrochim. Acta A 77 (2010) 73–81.
[44] D. Lin-Vien, N.B. Colthup, W.G. Fateley, J.G. Graselli, The Handbook of Infrared and Raman Characteristic Frequencies of Organic Molecules, Academic Press, Boston, MA, 1991.
[45] T. Rajamani, S. Muthu, Solid State Sci. 16 (2013) 90–101.
[46] N. Sundaraganesan, K. Satheshkumar, C. Meganathan, B.D. Joshua, Spectrochim. Acta A 65 (2006) 1186–1196.
[47] G. Socrates, Infrared and Raman Characteristic Group Frequencies, Tables and Charts, third ed., Wiley, Chichester, 2001.
[48] L.E. Fernandez, A.B. Altabef, A. Navarro, M. Fernandez, Gomez, E.L. Varetti, Spectrochim. Acta A 56 (2000) 1101.
[49] L.E. Fernandez, A.B. Altabef, E.L. Varetti, J. Mol. Struct. 612 (2002) 1–11.
[50] V. Krishnakumar, R. Ramasamy, Spectrochim. Acta A 69 (2008) 8–17.
[51] M. Arivazhagan, S. Jeyavijayan, Spectrochim. Acta A 79 (2011) 161–168.
[52] V. Krishnakumar, N. Prabavathi, Spectrochim. Acta A 77 (2010) 238–247.
[53] N. Puviarasan, V. Arjunan, S. Mohan, Turkey J. Chem. 26 (2002) 323.
[54] G. Varsanyi, Vibrational Spectra of Benzene Derivatives, Academic Press, New York, 1969.
[55] V. Krishnakumar, R.J. Xavier, Indian J. Pure Appl. Phys. 41 (2003) 597.
[56] M. Silverstein, G. Clayton Bassler, C. Morrill, Spectrometric Identification of Organic Compounds, Wiley, New York, 1981.
[57] M.K. Rofouei, N. Sohrabi, M. Shamsipur, E. Fereyduni, S. Ayyapan, N. Sundaraganesan, Spectrochim. Acta A 76 (2010) 182–190.
[58] N.P. Roeges, A Guide to complete Interpretation of Infrared Spectra of Organic Structures, Wiley, New York, 1994.
[59] G. Varsayani, Assigmentts for Vibrational Spectra of Seven Benzene Derivatives, vol. 1, Adam Hilger, London, 1974.
[60] E. Kavitha, N. Sundaraganesan, S. Sebastian, M. Kurt, Spectrochim. Acta A 77 (2010) 612–619.
[61] K. Chaitanya, Spectrochim. Acta A 86 (2012) 159–173.
[62] E. Kavitha, N. Sundaraganesan, S. Sebastian, Indian J. Pure Appl. Phys. 48 (2010) 20–30.
[63] A. Jayaprakash, V. Arjunan, S. Mohan, Spectrochim. Acta A 81 (2011) 620–630.
[64] S. Subashchandrabose, H. Saleem, Y. Erdogdu, G. Rajarajan, V. Thanikachalam, Spectrochim. Acta A 82 (2011) 260–269.
[65] T. Vijayakumar, I. Hubert Joe, C.P.R. Nair, V.S. Jayakumar, Chem. Phys. 343 (2008) 83–99.
[66] M. Govindarajan, M. Karabacak, A. Suvitha, S. Periandy, Spectrochim. Acta A 89 (2012) 137–148.